Neuron, Volume *74*

Supplemental Information

The p150^{Glued} CAP-Gly Domain Regulates Initiation of Retrograde Transport at Synaptic Termini

Thomas E. Lloyd, James Machamer, Kathleen O'Hara, Ji Han Kim, Sarah E. Collins, Man Y. Wong, Brooke Sahin, Wendy Imlach, Yunpeng Yang, Edwin S. Levitan, Brian D. McCabe, and Alex L. Kolodkin

Figure S1

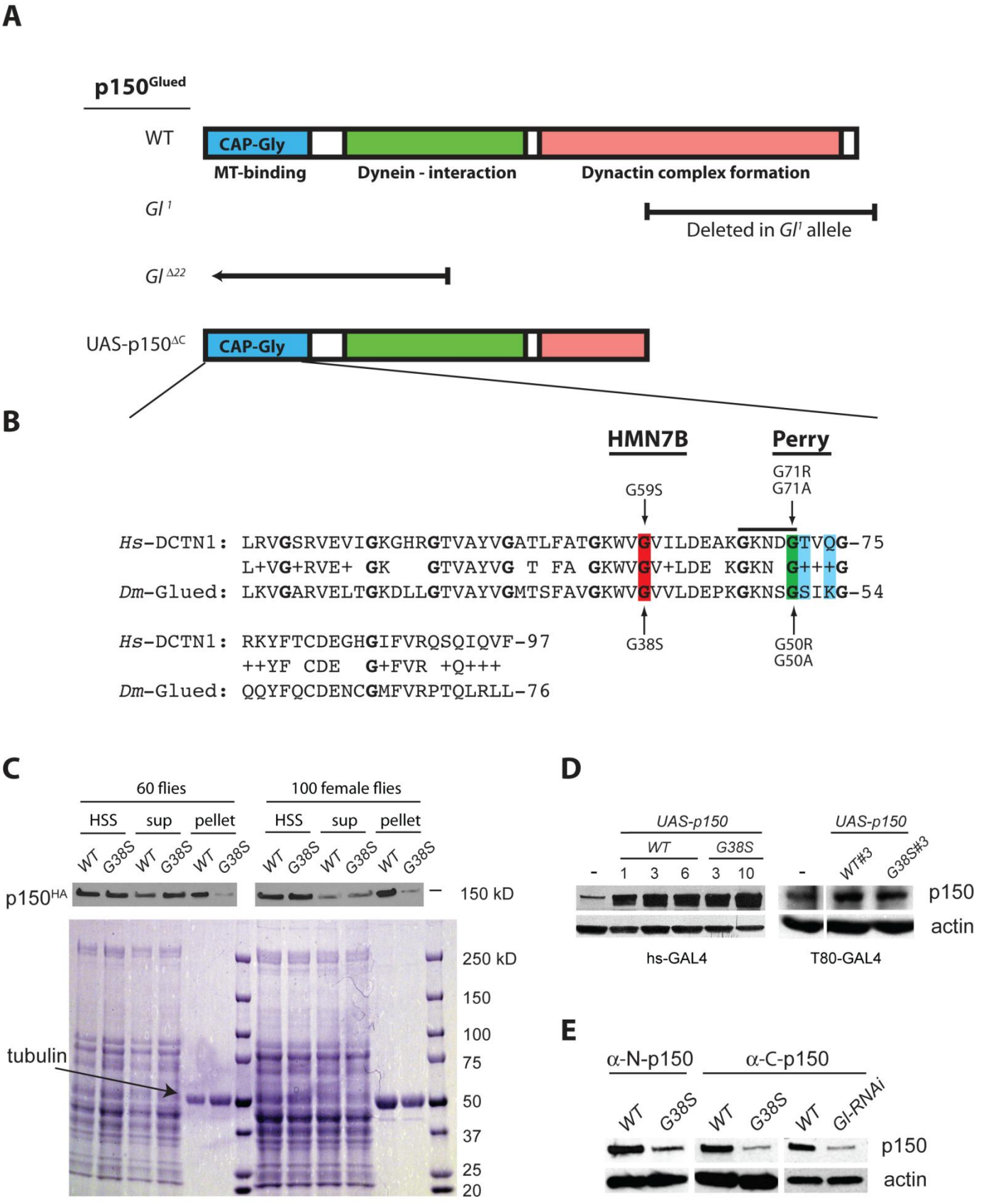
A
p150Glued
WT
CAP-Gly
MT-binding
Dynein - interaction
Dynactin complex formation
Gl 1
Deleted in Gl1 allele
Gl Δ22
UAS-p150ΔC
CAP-Gly
B
HMN7B
Perry
G59S
G71R
G71A
Hs-DCTN1: LRVGSRVEVIGKGHRGTVAYVGATLFATGKWVGVILDEAKGKNDGTVQG-75
L+VG+RVE+ GK GTVAYVG T FA GKWVGV+LDE KGKN G+++G
Dm-Glued: LKVGARVELTGKDLLGTVAYVGMTSFAVGKWVGVVLDEPKGKNSGSIKG-54
G38S
G50R
G50A
Hs-DCTN1: RKYFTCDEGHGIFVRQSQIQVF-97
++YF CDE G+FVR +Q+++
Dm-Glued: QQYFQCDENCGMFVRPTQLRLL-76
C
60 flies
100 female flies
HSS
sup
pellet
WT
G38S
p150HA
150 kD
250 kD
150
100
75
50
37
25
20
tubulin
D
UAS-p150
WT
G38S
-
1
3
6
3
10
UAS-p150
-
WT#3
G38S#3
p150
actin
hs-GAL4
T80-GAL4
E
α-N-p150
α-C-p150
WT
G38S
WT
G38S
WT
Gl-RNAi
p150
actin

Figure S1, related to Figure 1. Mutations in *Drosophila* CAP-Gly Domain of p150^{Glued}

(A) Domain structure and existing alleles of *Drosophila p150^{Glued}*. The *Gl^{1}* allele is a dominant-negative allele generated by a 9kb roo element insertion in the 3' end of the gene and resulting in a truncated transcript (Swaroop et al., 1985). The transgenic line *UAS-p150$^{\Delta C}$* overexpresses this C-terminal truncated protein (Allen et al., 1999). The Cytoskeletal-associated protein, glycine rich (CAP-Gly) microtubule (MT) binding domain (blue), and the dynein-interaction domain (green) remain intact in these mutant proteins. *Gl$^{\Delta 22}$* is a null allele generated by imprecise P-element excision (Siller et al., 2005). (B) Conservation and mutations of the CAP-Gly domain. Alignment of *Drosophila melanogaster* (*Dm*) p150^{Glued} and *Homo sapiens* (*Hs*) p150^{Glued} (DCTN1) CAP-Gly domains. These domains are ~60% identical and 80% similar (BLAST). (+) indicates amino acid similarity. The residues mutated in human diseases are colored (red is HMN7B mutation; green indicates most common residue mutated in Perry Syndrome and blue indicates other residues mutated in Perry Syndrome), and the mutations described in this study are indicated with an arrow. Note that *Glued^{G38S}* in *Drosophila* is equivalent to p150^{G59S} in humans/mice. The line indicates the highly conserved GKNDG motif present in all CAP-Gly domains that is implicated in binding to proteins containing EEY/F at their carboxy termini. (C) p150^{G38S} has impaired association with microtubules in vivo. High speed supernatant (HSS) of fly extracts from flies overexpressing HA-tagged p150 (WT or G38S) under control of *hs-GAL4* were incubated with taxol and GTP to stabilize microtubules, and microtubule associated proteins were isolated by ultracentrifugation through a 15% sucrose cushion. Equal fractions of each sample were loaded on gels to perform Western analysis for p150^{HA} with anti-HA antibody (top) and also stained with Coomasie (bottom) to demonstrate purification of microtubules in the pellet. The intensity of the anti-HA signal is ~8x higher in the pellet from WT extracts compared

with G38S (quantitated using ImageJ), whereas the intensity of anti-HA signal in the supernatant (sup) is ~ 1.5x higher in G38S extracts. These data suggest that the ratio of microtubule bound:solube p150 is ~12x higher in $p150^{WT}$ than $p150^{G38S}$. (D) Expression of untagged *UAS-p150* transgenes using *hs-GAL4* (left) and *T80-GAL4* (right). To circumvent the toxicity of constitutive ubiquitous overexpression of p150, *UAS-p150* transgenic animals were crossed to *hs-GAL4*, and third-instar larvae were heat shocked for one hour at 37 °C and protein extracted 16 hours later. Expression of *UAS-p150* transgenes in 0-3 day old adult flies using *T80-GAL4*, a low level ubiquitous *GAL4* driver, shows that *UAS-$p150^{WT}$[#3]* and *UAS-$p150^{G38S}$[#3]* transgenes express p150 proteins at similar levels and are used in this study. (**E**) Western analysis of p150 in *Gl^{G38S}* fly heads demonstrates a reduction in p150 protein levels using antibodies directed against both the C- and N-terminus, similar to the effect of *Glued* RNAi (*$elav^{C155}$/UAS-Glued-RNAi*).

Figure S2

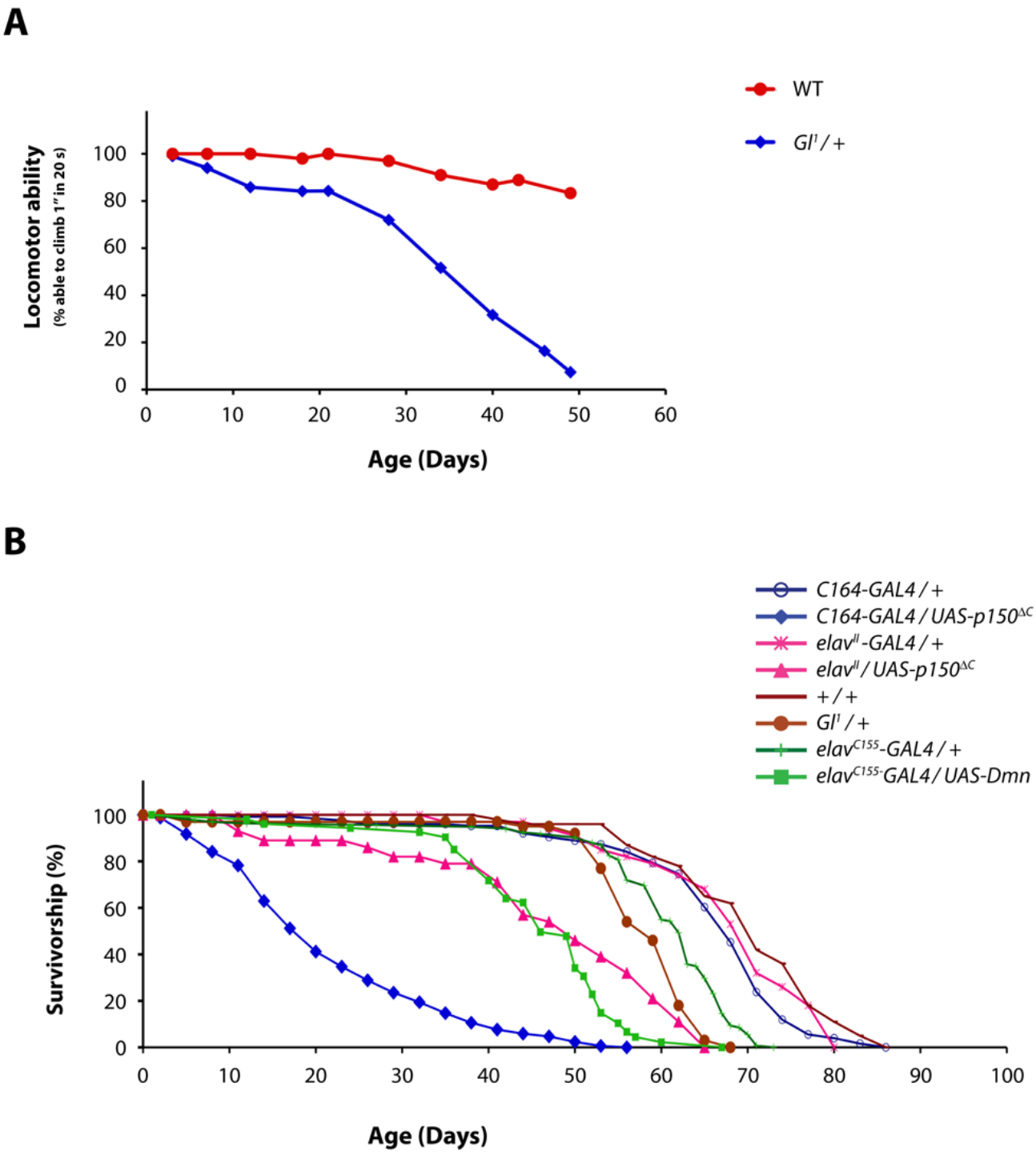
A
WT
Gl¹ / +
Locomotor ability
(% able to climb 1" in 20 s)
100
80
60
40
20
0
0
10
20
30
40
50
60
Age (Days)
B
C164-GAL4 / +
C164-GAL4 / UAS-p150ΔC
elavII-GAL4 / +
elavII / UAS-p150ΔC
+ / +
Gl¹ / +
elavC155-GAL4 / +
elavC155-GAL4 / UAS-Dmn
Survivorship (%)
100
80
60
40
20
0
0
10
20
30
40
50
60
70
80
90
100
Age (Days)

Figure S2, related to Figure 1. Disruption of Glued in neurons causes progressive locomotor dysfunction and early lethality

(A) *Glued*^{1} heterozygous flies (isogenized in the w^{1118} background by backcrossing six generations) develop progressive locomotor dysfunction with age as compared to wild-type (w^{1118}) control flies. (B) Disruption of *Glued* causes decreased lifespan. *Glued*^{1} heterozygous flies have decreased lifespan relative to control flies. Overexpression of p150$^{\Delta C}$ or dynamitin (Dmn) in motor neurons (using *C164-GAL4*) or all neurons (*elav*^{II}*-GAL4* or *elav*^{C155}*-GAL4*) causes shortened lifespan. *C164* may cause a more severe phenotype than *elav*^{II} due to stronger expression in motor neurons. *elav*^{C155} is a stronger panneuronal driver than *elav*^{II}.

Figure S3

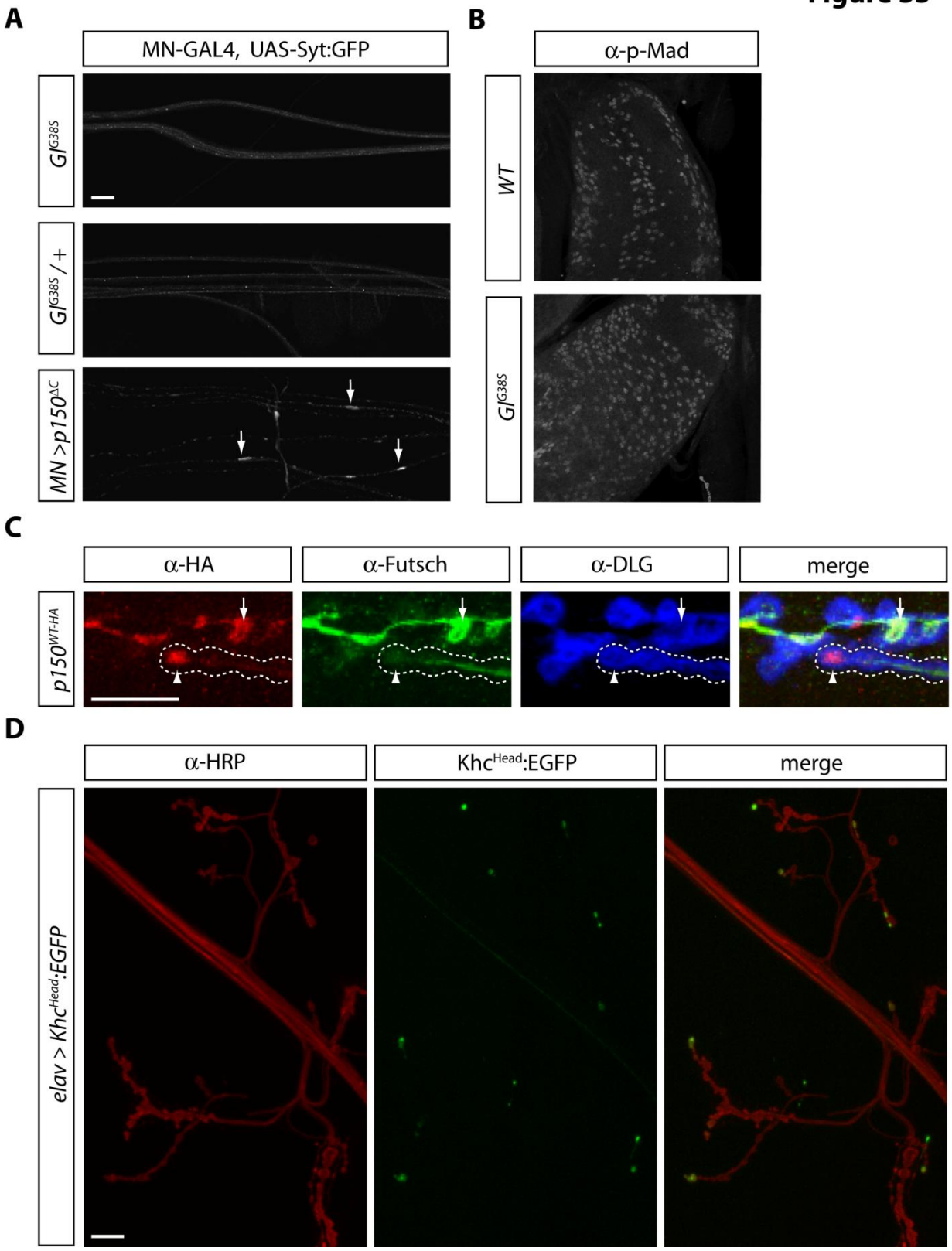
A
MN-GAL4, UAS-Syt:GFP
GI^G38S
GI^G38S / +
MN >p150^ΔC
B
α-p-Mad
WT
GI^G38S
C
α-HA
α-Futsch
α-DLG
merge
p150^WT-HA
D
α-HRP
Khc^Head:EGFP
merge
elav > Khc^Head:EGFP

Figure S3, related to Figure 2. Normal axonal transport and retrograde endosomal signaling in Gl^{G38S} animals, and $p150^{Glued}$ is enriched at microtubule (+) ends of NMJ TBs. (A) Axonal jams of Synaptotagmin:GFP (Syt:GFP) are observed with overexpression of dominant-negative *Glued* ($p150^{\Delta C}$) in motor neurons using *D42-GAL4*, but not in Gl^{G38S} animals; no difference in Syt:GFP is observed between Gl^{G38S} heterozygous and homozygous axons. "MN-GAL4" is motor neuron-GAL4 (*C164* for overexpression of UAS-Syt:GFP and *D42* for overexpression of $p150^{\Delta C}$) (B) pMad levels in motor neuron nuclei are normal in Gl^{G38S} animals. (C) $p150^{WT-HA}$ is enriched at terminal boutons (enlarged region of Figure 2A). $p150^{WT-HA}$ protein is expressed in motor neurons (*OK371*) and labeled using anti-HA antibody (red). Stable microtubule bundles are labeled using antibodies to the microtubule-associated protein Futsch (green), and the post-synaptic density is labeled with antibodies to DLG. Microtubule loops (indicated by the arrow), believed to contain free microtubule (+) ends (Roos and Kelly, 2000), are enriched in p150. A type Is NMJ is outlined. (D) Terminal boutons are enriched in microtubule (+) ends. Neuronal expression of Khc^{Head}:EGFP to label microtubule (+) ends demonstrates that microtubule (+) ends are markedly enriched at terminal boutons. *elav-GAL4* was used at 18°C to provide low level expression, as high level expression causes severe axonal transport disruption and early larval lethality. See also Movie S3. Scale bar = 10 μm.

Figure S4

A

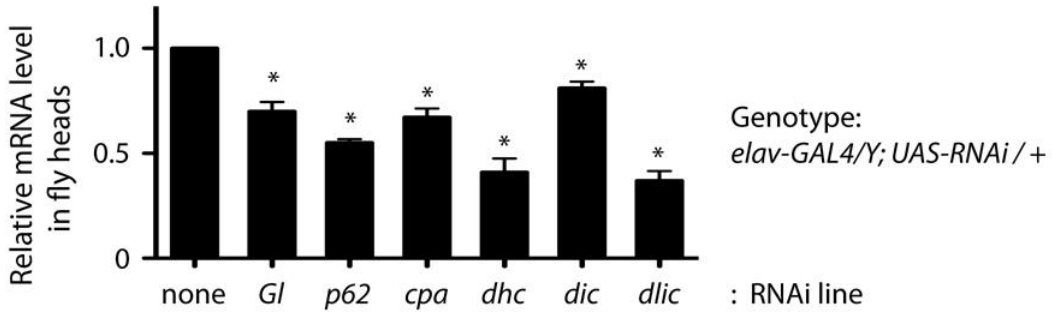
Relative mRNA level in fly heads
1.0
0.5
0
*
none
Gl
p62
cpa
dhc
dic
dlic
: RNAi line
Genotype:
elav-GAL4/Y; UAS-RNAi / +

B

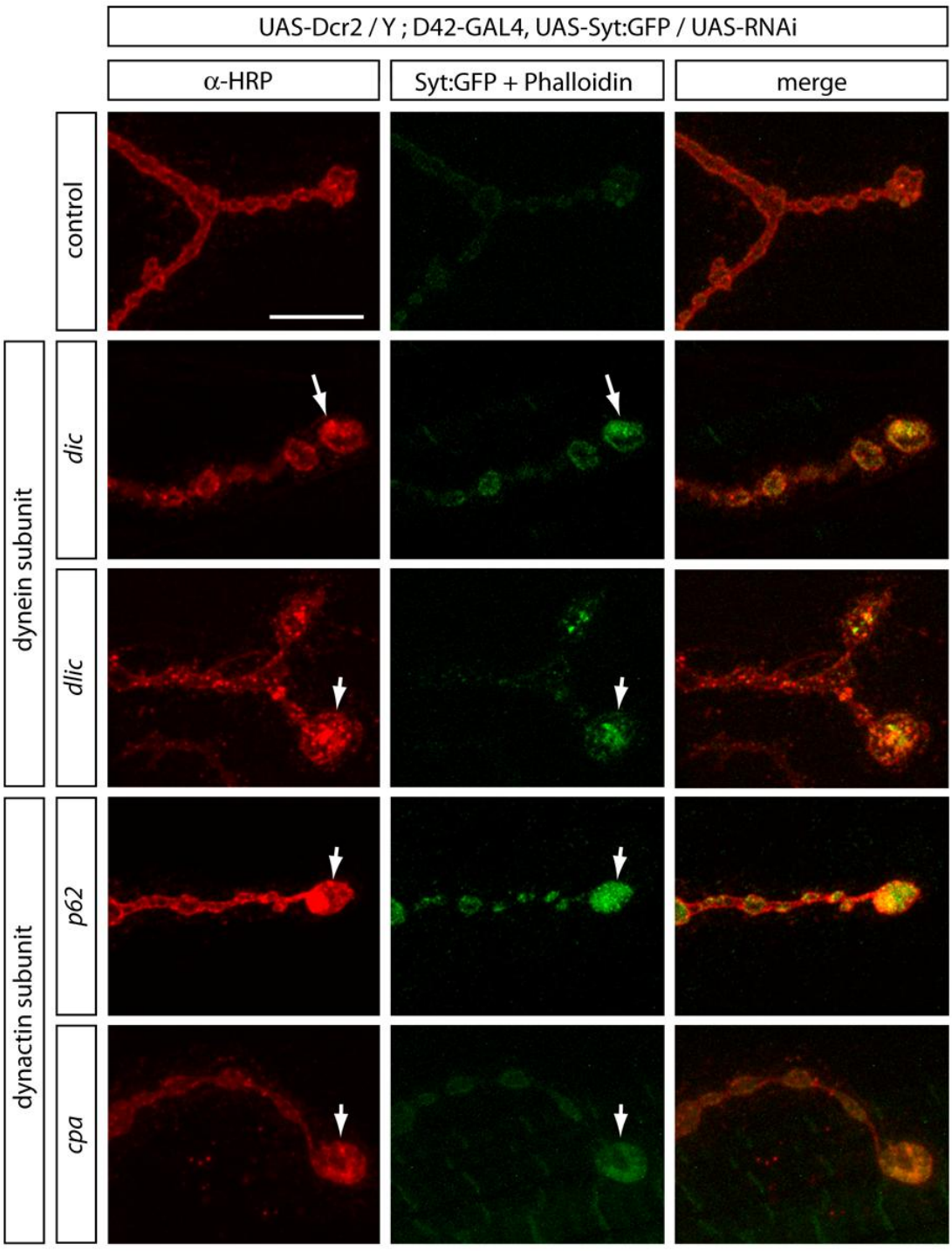
UAS-Dcr2 / Y ; D42-GAL4, UAS-Syt:GFP / UAS-RNAi
α-HRP
Syt:GFP + Phalloidin
merge
control
dynein subunit
dic
dlic
dynactin subunit
p62
cpa

Figure S4, related to Figure 3. Knockdown of multiple dynein/dynactin subunits with RNAi in motor neurons phenocopies *Glued* terminal bouton phenotypes

(A) Quantitation of RNAi knockdown in neurons using qRT-PCR. mRNA levels were determined from fly heads of *elav*^{C155}*-GAL4* /Y; *UAS-RNAi/+* flies. Note that the quantitation markedly underestimates the knockdown effect seen in B (and Figure 3C and 3E) since neuronal mRNA comprises only a fraction of total fly head mRNA. Samples were run in triplicate in at least 3 independent experiments. RNAi-mediated knockdown of *cpa* and *dlic* at 25 °C was lethal, and therefore these experiments were carried out at 18 °C for these two lines. * $p < 0.01$ in a one sample t-test with theoretical mean 1.0. (B) Knockdown of dynein subunits (*Dynein intermediate chain (dic)* and *Dynein light intermediate chain* (*dlic)*) and dynactin subunits (*capping protein alpha* (*cpa)* and *p62*) show terminal bouton accumulations of α-HRP and synaptotagmin (Syt:GFP) (arrow). FITC-conjugated phalloidin was used to label muscles for segment identification. Scale bar = 10 μm.

Figure S5

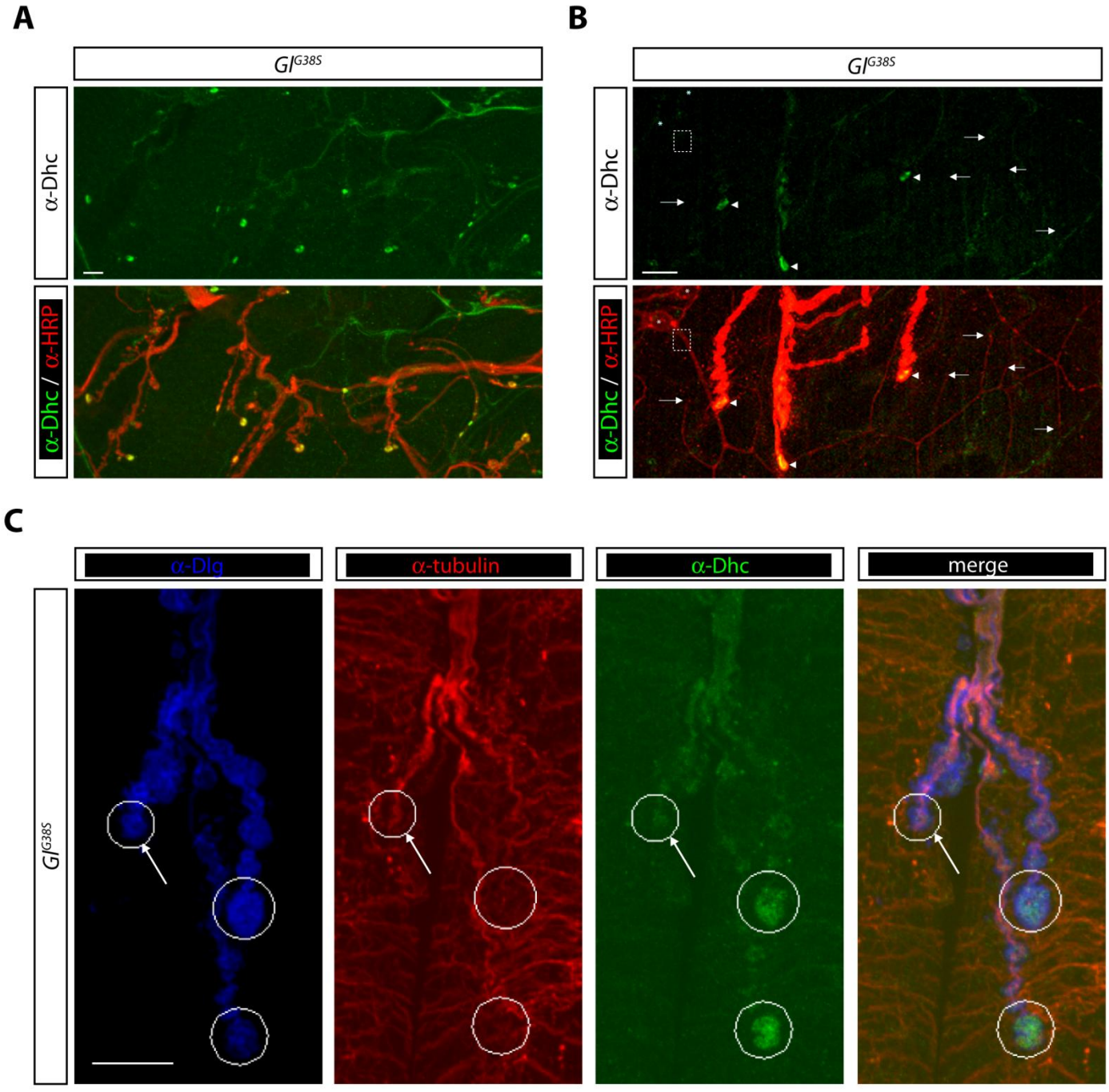

Figure S5, related to Figure 4. Dhc accumulates at terminal boutons at the NMJ, but not in dendrites in *Gl*^{G38S} animals

(A) An A3 hemisegment of a *Gl*^{G38S} larval body wall labeled with α-Dhc and α-HRP shows that in NMJs with multiple branches, Dhc preferentially accumulates in mutant terminal boutons of the distal-most branch. (B) Dhc accumulates at terminal boutons of the NMJ (arrowheads) in *Gl*^{G38S} larvae, but not in dendrites. Arrows show the distal tips of dendrites (labeled in red) that are (-) end out in *Drosophila*, and the box shows a proximal base of a dendrite: the location of dendritic microtubule (+) ends. (C) Dhc does not accumulate in *Gl*^{G38S} terminal boutons (circled) in which microtubule bundles are observed (arrow); rather Dhc accumulates preferentially in terminal boutons with reduced levels of tubulin staining. Scale bar = 10 μm.

Figure S6

A

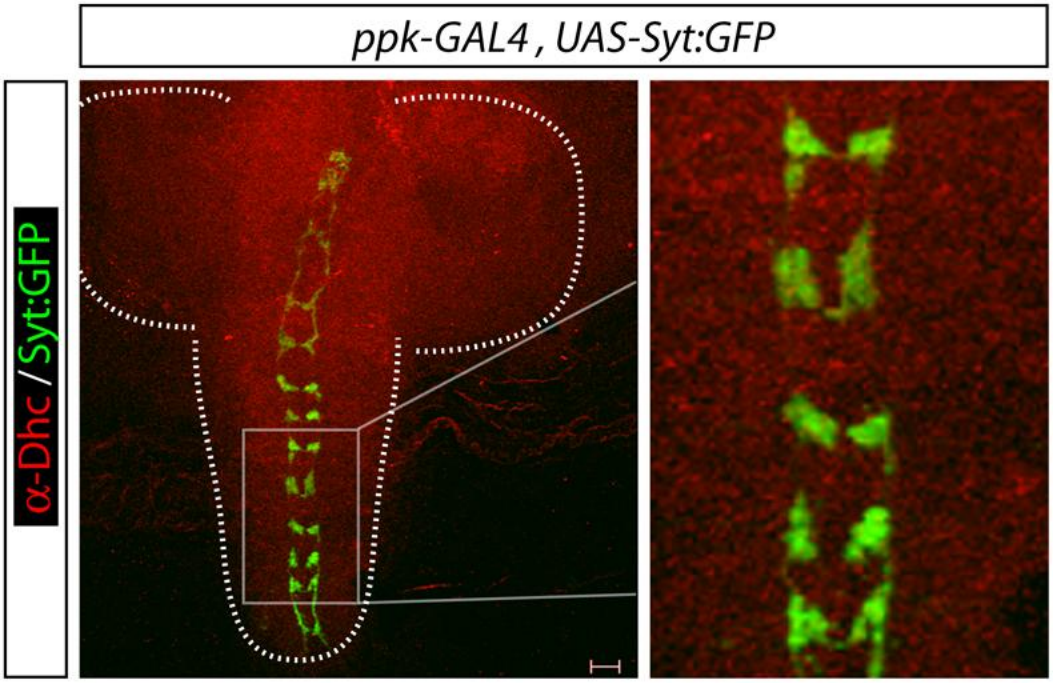
ppk-GAL4 , UAS-Syt:GFP
α-Dhc / Syt:GFP

B

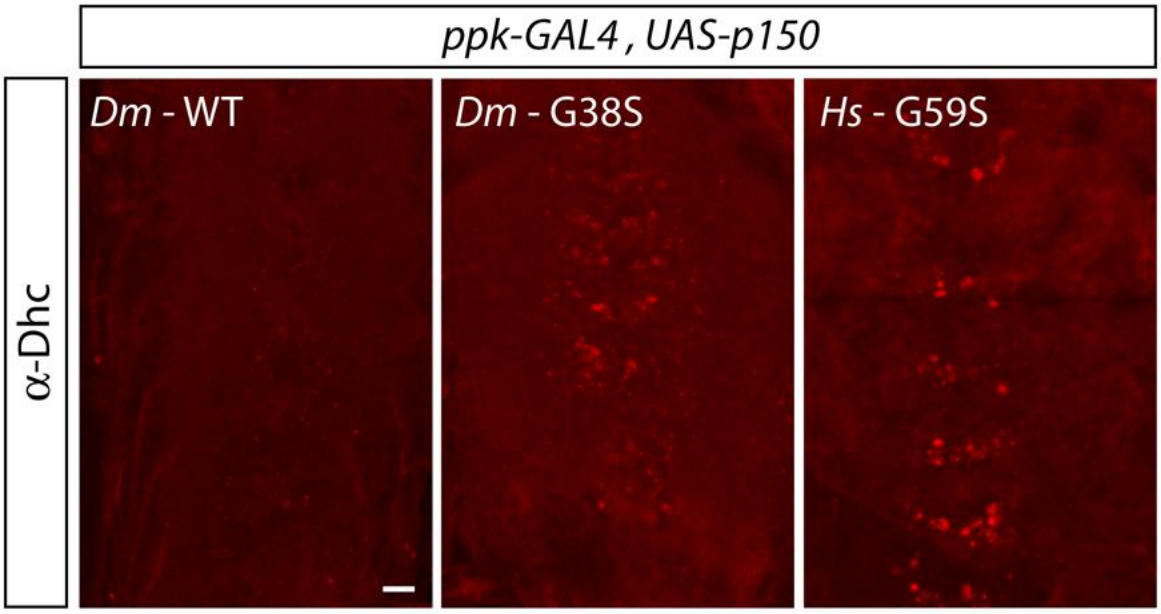
ppk-GAL4 , UAS-p150
α-Dhc
Dm - WT
Dm - G38S
Hs - G59S

Figure S6, related to Figure 4. Dhc accumulates at sensory synaptic termini with overexpression of mutant p150

(A) Overexpression of synaptotagmin:GFP in multidendritic sensory neurons with *ppk-GAL4* labels synapses of these neurons within the larval CNS neuropil. Right panel enlargement highlights the stereotyped ladder-like pattern of synapses. (B) Overexpression of p150 in sensory neurons shows a marked accumulation of Dhc within synaptic termini following overexpression of mutant *Drosophila* (*Dm* – G38S) or human (*Hs* – G59S), but not wild-type (*Dm* –WT) protein. Scale bar = 10 μm (A) or 5 μm (B).

Figure S7

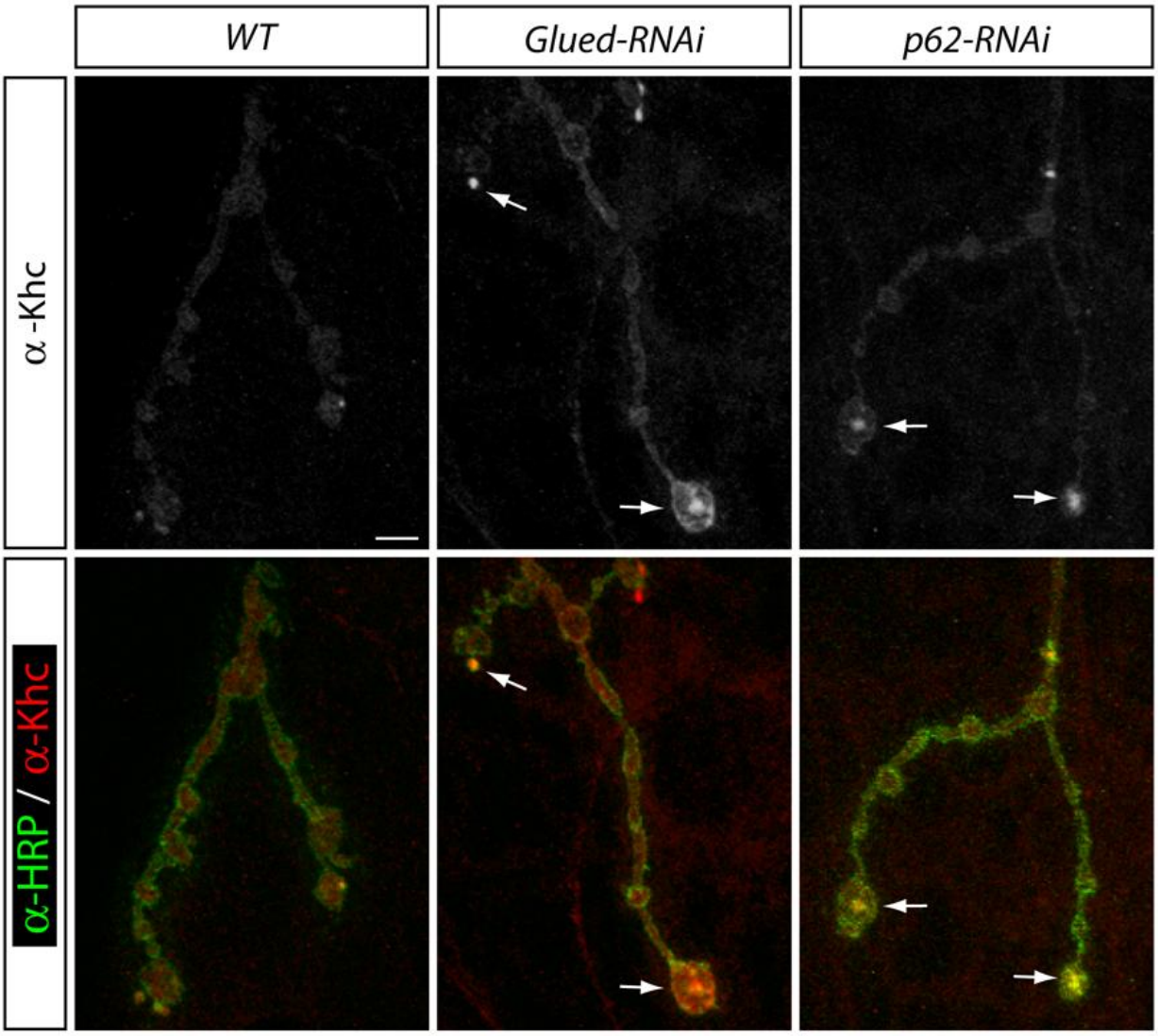

Figure S7, related to Figure 5. Khc accumulates at terminal boutons with RNAi-mediated knockdown of dynactin subunits p150^{Glued} and p62

Larval NMJs overexpressing RNAi for *Glued* or *p62* show marked terminal bouton accumulations of Khc (arrows). Scale bar = 5 μm.

Figure S8

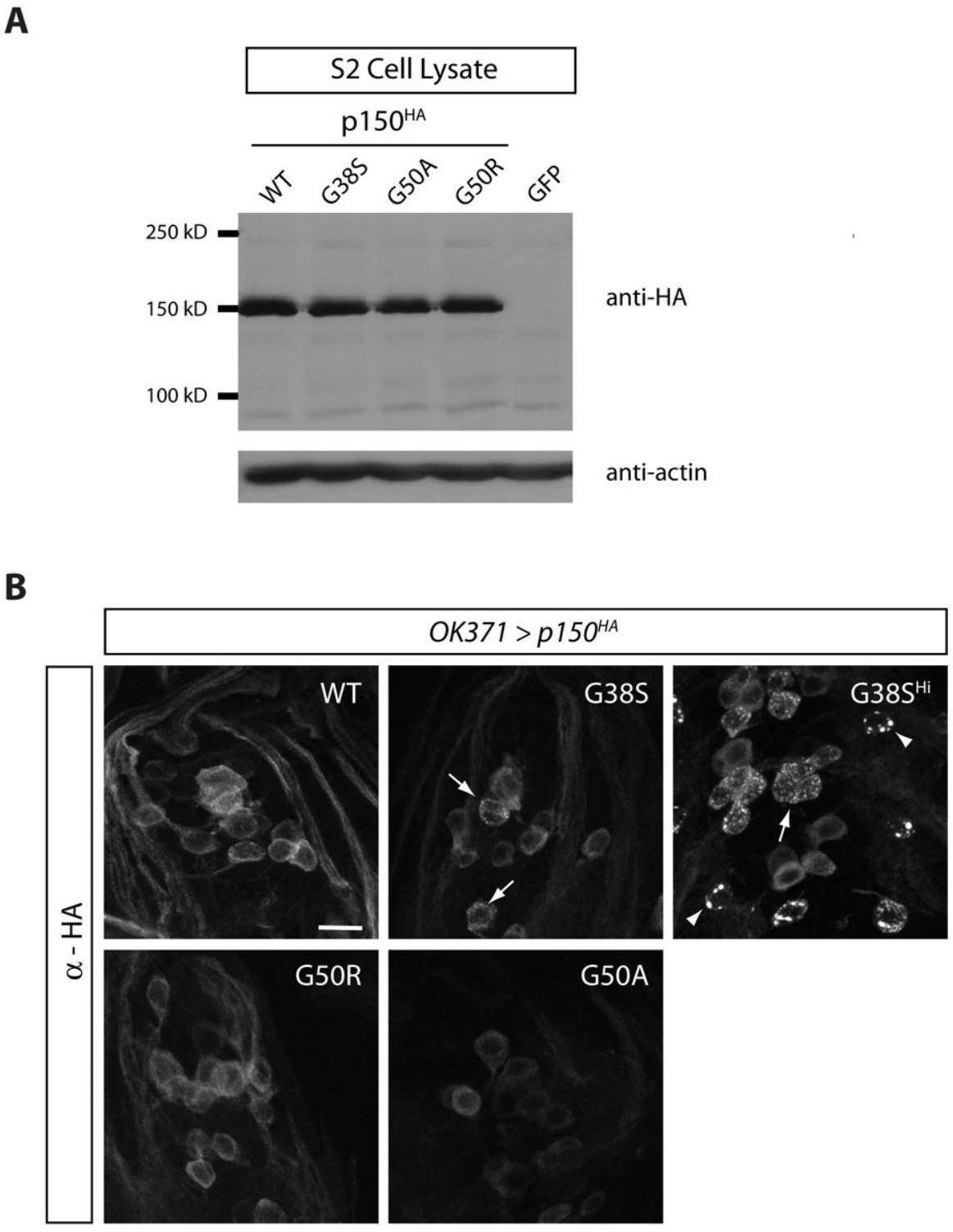
A
S2 Cell Lysate
p150HA
WT
G38S
G50A
G50R
GFP
250 kD
150 kD
100 kD
anti-HA
anti-actin
B
OK371 > p150HA
α - HA
WT
G38S
G38SHi
G50R
G50A

Figure S8, related to Figure 7. HMN7B, but not Perry, mutant p150 proteins form cytoplasmic aggregates within motor neurons

(A) HA-tagged $p150^{WT}$, $p150^{G38S}$, $p150^{G50A}$, and $p150^{G50R}$ proteins are expressed at similar levels in S2 cells. Anti-actin is used to control for protein loading. (B) HA-tagged $p150^{WT}$, $p150^{G50A}$, and $p150^{G50R}$ are diffusely expressed in the cytoplasm of motor neuron cell bodies and in axons with *OK371-GAL4*; whereas $p150^{G38S}$ overexpression forms cytoplasmic punctae (arrows), which are often quite large in the high-level expressing line ($G38S^{Hi}$) (arrowheads). Scale bar = 10 μm.

SUPPLEMENTAL EXPERIMENTAL PROCEDURES

Generation of transgenic lines

UAS-p150^{WT} and *UAS-p150^{G38S}* were generated by excising the *Drosophila* p150 cDNA from pBluescript and directionally cloning into *pUAST*. C-terminal HA-tagged constructs were generated using PCR and cloned into *pUASTattB* (Bischof et al., 2007). ORFs were fully sequenced to ensure that plasmids contained only the desired mutation. The line *BAC {Gl+}* was generated by injecting the purified BAC (*CH322- 82J07*, *CHORI BACPAC* Resource Center) into strain *yw*; *PBac{y^{+}-attP-9A}tmodVK^{00020}* (Venken et al., 2009). Transgenic animals were generated by injection (Genetics Systems, Boston MA, or Best Gene Inc, Chino Hills, CA). The *G38S^{Hi}* line was identified as a transgenic *pUASTattB* line with a dark eye color, suggesting that there are multiple insertions of the P element.

Generation of *Gl^{G38S}* knock-in allele

The 5' arm was generated by PCR amplifying a 3.8 kb genomic fragment of the *Glued* locus from *BAC RP98-48C4* (CHORI BACPAC) and introducing the G38S mutation using site-directed mutagenesis as described above (this mutation introduces an HphI site used to select for the mutation). A 3.8 kb 3' arm flanked by the I-SceI site (within the first intron of the *Glued* gene) was also PCR amplified from genomic DNA, and the two fragments cloned into the NotI site of the pTV2 vector (Rong et al., 2002) to generate *pTV2-Gl^{G38S}*. This construct was injected into *w^{1118}* embryos to obtain P{donor-*Gl^{G38S}*} on chromosome II (see Figure 1). This line was crossed to *yw; P{70FLP}11 P{70I-SceI}2B/CyO* and treated with heat shock to generate two double-stranded breaks. Approximately 1000 single virgin females with mosaic eye color were

crossed to *w; P{70FLP}10*, and a single w^+ insertion that mapped to chromosome III was obtained (*Dp* {*Gl, P{*w^+*,* Gl^{G38S}*}*}), demonstrating stable transfer of the w^+ marker from the second chromosome to the third. Linkage of the w^+ marker with the *Glued* locus was confirmed by lack of recombination with Gl^1, and duplication of the *Glued* locus was confirmed using Southern analysis using the *glued* cDNA as probe, and then sequencing confirmed the presence of the G38S mutation. *Dp* (*Gl, P{*w^+*,* Gl^{G38S}*}*) was crossed to *hs-Cre*, allowing resolution of the tandem duplication, and reduced alleles were identified by loss of the w^+ marker. Approximately 10 independent w^- lines were generated, and most of these lines failed to complement $Gl^{\Delta 22}$. The presence of the G38S mutation was confirmed by sequencing genomic DNA from several lines, and resolution of the duplication was confirmed by Southern analysis. One line (Gl^{G38S}) was recombined for six generations with Canton-S to remove second-site mutations (in each generation, the mutation was selected by HphI digestion).

Additional Fly Strains

$elav^{C155}$*>ANF:GFP* and *elavGS>ANF:GFP* are described in Wong et al., 2012. *C164-GAL4* (Torroja et al., 1999) was provided from Hugo Bellen. The *OK371-GAL4*, *UAS-mCD8:GFP* line expressing plasma membrane targeted GFP in motor neurons was a gift from H. Aberle (Mahr and Aberle, 2006). *P{Mhc.CD8-GFP-Sh}* was obtained from C.S. Goodman. *UAS-*$p150^{\Delta C}$ was obtained from Rod Murphey (Allen et al., 1999). *UAS-RNAi* lines were provided from the VDRC (*dic*: P{GD17212}v48334, *dlic*: P{GD9681}v41686, *cpa*: P{KK108554}v100773, *p62*: P{GD7465}v31623, and *Gl*: P{GD1455}v3785) and Bloomington Stock Center (*khc*: *P{TRiP.JF01939}attP2* and *dhc*: *P{TRiP.JF03177}attP2*. Other fly stocks used in this study were obtained from the Bloomington stock center including the khc^8 allele,

UAS-Khc^{Head}*:GFP*, *UAS-Dynamitin*, *UAS-APP:YFP*, *UAS-Syt:eGFP,* UAS-Dcr-2 (on X) and GAL4 lines: *D42=P{GawB}D42*, *elav* (*elav*^{C155}*=P{GawB}elav*^{C155}*; elav*^{II} *= P{GAL4-elav.L}2, and elav =P{GAL4-elav.L}3E*), *T80=P{GawB}T80/CyO*, *OK371 = P{GawB}VGlut*^{OK371}, *hs =* P{GAL4-*Hsp70.PB}2*, and *daughterless=P{GAL4-da.G32}UH1*. *UAS-Khc-EGFP* (on II) expresses the head domain of Khc (a SphI-BstI fragment corresponding to bases 248-2134 of the GenBank sequence) fused to EGFP sequence and was generated by Patty Estes and obtained from Bloomington.

Locomotor and Lethality Assays

The larval locomotor assay was performed as described (Batlevi et al., 2010). For adult assays, twenty female flies per vial that were carefully age-matched by collecting progeny within two days of eclosion were maintained at 25 °C, and surviving flies were transferred to fresh vials every other day. Locomotor function was tested every 3 to 4 days by tapping flies to the bottom of a vial and counting the number of flies able to climb 1 inch in 20 seconds.

Antibodies

Ms anti-Dhc (P1H4) was provided by Tom Hays (McGrail et al., 1995) and used at 1:250. Total protein expression levels were determined using Western blot analysis on total fly extracts with anti-Ct-dp150 or anti-Nt-dp150 antibody (Kim et al., 2007), and blots were stripped and reprobed with anti-actin (Santa Cruz) to ensure equal loading. Immunohistochemistry was performed on filleted third-instar larvae using the following antibodies: 4F3 (DLG 1:250), 22C10 (Futsch 1:100), and nc82 (Brp 1:100) (Developmental Studies Hybridoma Bank), rabbit (1:1000) or mouse (3E6, 1:250) anti-GFP (Molecular Probes), rabbit anti-pMad (41D10, Cell

signaling, 1:25), rabbit anti-Khc (Chemicon, 1:100), rat monoclonal anti-HA (3F10, 1:100), rabbit anti-HRP (Jackson ImmunoResearch, 1:1000), and goat anti-HRP (DyLight 549- or Cy5-conjugated, Jackson ImmunoResearch 1:250). Alexa488-, Alexa546-, or Alexa647-conjugated goat secondary antibodies were used (Molecular Probes, 1:250).

Live imaging and image analysis

For axonal transport analysis of Rab7:GFP, nerves distant from the ventral nerve cord (in the posterior section of the larvae) were imaged at room temperature within 20 minutes of dissection. GFP fluorescence was acquired at frame rate of 2 Hz for 1 minute and at a resolution of 1388 X 1040. Analysis was performed using ImageJ and excel macros as described (Louie et al., 2008). Rab7:GFP vesicles tracked for analysis were randomly chosen independent of their dynamic characteristics, but were included only if they could be tracked for at least 60 frames. We defined the start of a run by a minimal displacement of 0.2 μm/s and the end of a run by a minimal displacement of 0.08 μm /s. 7 animals per genotype and 12-48 particles per animal were analyzed. A vesicle was considered stationary if runs were <5% of the imaging duration and the vesicle had a total displacement of < 0.5 μm.

For ANF:GFP imaging from TBs, 4 optical planes per time point were imaged at a rate of ~0.5 s per confocal stack. A maximum projection of this stack was used to count the number of vesicles exiting the terminal bouton in ~6.5 minutes. The rate of vesicle trafficking from the TB was determined by dividing the total number of boutons leaving by the time of imaging.

For fixed samples, different genotypes were stained simultaneously and in the same tube when possible. Quantitation was performed blinded to genotype. Images of different genotypes were acquired sequentially using identical confocal settings. Data from 4 proximal segments

(A2 and A3) and 4 distal segments (A5 and A6) were averaged for each animal.

Quantitative RT-PCR

30 fly heads, age 0-2 days old, were collected and frozen on dry ice. RNA was extracted using TRIzol Reagent (Invitrogen) and homogenized using a pellet pestle (Kimble-Kontes, Vineland, NJ). 1 ug of total RNA was reverse transcribed to cDNA using High-Capacity cDNA Reverse Transcription Kit (ABI). qRT-PCR was performed, in triplicate, using Applied Biosystems Gene Expression Master Mix on an Applied Biosystems 7900HT machine. TaqMan® control primer for RpL32, (Dm02151827_g1) and experimental primer for *glued* (Dm01822734_g1), *cpa* (Dm01827763_g1), *p62* (Dm01815980_s1), *dhc* (Dm01822118_g1), *dic* (Dm01799704_g1), *dlic* (Dm01825336_g1) were used. Relative Quantitation was performed using the comparative CT method (ABI manual).

S2 Cell Culture

S2R+ cells were grown in Gibco Schneider's Drosophila medium supplemented with 2 mM L-Glutamine, 10%FBS, penicillin (100 U/mL) and streptomycin (100 μg/mL). Cells were seeded/plated at 0.5 X 10^6 cells/well in a standard 24 well plate on untreated glass coverslips. Cells were transfected 24 hours later with 0.1 ug β-Actin Gal4 and 0.1 ug experimental DNA according to the Qiagen Effectene protocol. Cells were then grown for 24-48 hours and processed for immunohistochemistry or Western analysis.

Electrophysiology

Wandering third instar larvae were dissected in HL3 (Stewart et al., 1994) containing 0.2 mM Ca2+, and recordings were carried out in HL3 with 1 mM Ca2+. Recordings where the resting membrane potential was less than −55 mV were discarded. Sharp electrodes (~ 30 MW) were filled with 3M KCL. Suction electrodes were filled with HL3 + 1mM Ca2+. Stimulation was induced by a Master 8 pulse generator (AMPI). Responses were detected with an Axon HS-2A head stage and an Axoclamp 2B amplifier; data were low-pass filtered at 1 kHz, digitized, and recorded to disk with a Digidata 1322A interface using Clampex v 8.2.0.235 (Axon Instruments). mEJP's were analysed using Mini analysis software (Synaptosoft, v 6.0.3).

SUPPLEMENTAL REFERENCES

Batlevi, Y., Martin, D.N., Pandey, U.B., Simon, C.R., Powers, C.M., Taylor, J.P., and Baehrecke, E.H. (2010). Dynein light chain 1 is required for autophagy, protein clearance, and cell death in Drosophila. Proceedings of the National Academy of Sciences of the United States of America *107*, 742-747.

Mahr, A., and Aberle, H. (2006). The expression pattern of the Drosophila vesicular glutamate transporter: a marker protein for motoneurons and glutamatergic centers in the brain. Gene Expr Patterns *6*, 299-309.

Stewart, B.A., Atwood, H.L., Renger, J.J., Wang, J., and Wu, C.F. (1994). Improved stability of Drosophila larval neuromuscular preparations in haemolymph-like physiological solutions. J Comp Physiol A *175*, 179-191.

Torroja, L., Packard, M., Gorczyca, M., White, K., and Budnik, V. (1999). The Drosophila beta-amyloid precursor protein homolog promotes synapse differentiation at the neuromuscular junction. J Neurosci *19*, 7793-7803.

Venken, K., Carlson, J.W., Schulze K.L., Pan, H., He, Y., Spokony, R., Wan, K.H., Koriabine, M., de Jong, P.J., White, K.P., *et al.* (2009). Versatile P[acman] BAC Libraries for transgenesis studies in Drosophila melanogaster. Nature methods *6*, 431-4.